Biophysical Chemistry 254 (2019) 106243

Contents lists available at ScienceDirect

Biophysical Chemistry

journal homepage: www.elsevier.com/locate/biophyschem

How the dyes affect folding of small proteins in single-molecule FRET experiments: A simulation study

Sergei F. Chekmarev[a,b]

[a] Institute of Thermophysics, SB RAS, 630090 Novosibirsk, Russia
[b] Department of Physics, Novosibirsk State University, 630090 Novosibirsk, Russia

HIGHLIGHTS

- Comparative simulation study of folding of BBL protein and two of its FRET constructs.
- Dyes and their positions do not significantly affect the overall picture of folding.
- In all cases, folding kinetics are two-state but the FRET constructs fold slower.
- Repulsive interaction of dyes with protein is essential to reproduce BBL folding.

GRAPHICAL ABSTRACT

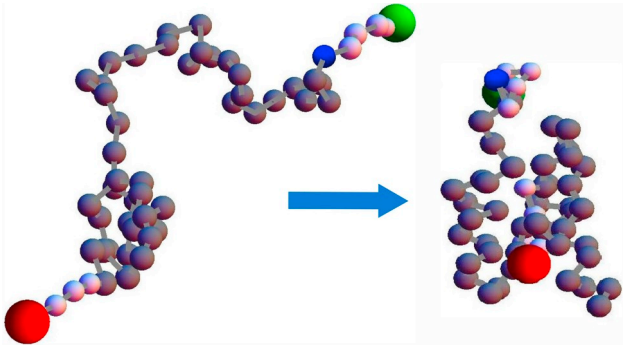

ARTICLE INFO

Keywords:
Protein folding
Single-molecule Förster resonance energy transfer (smFRET)
Dye positions
Free energy surfaces
Folding times
FRET efficiency histograms

ABSTRACT

A key question in the application of the single-molecule Förster resonance energy transfer (smFRET) technique to study protein folding is how the dyes affect the protein behavior. Understanding of these effects is particularly important for small proteins, for which the dyes, along with their linkers, can be comparable in size (mass) with the protein. Using a coarse-grained model, we simulated folding of BBL protein and two of its FRET constructs. The obtained results suggest that even for small proteins, such as the 45-residue BBL, the appearance of the excluded volume in the protein conformation space due to the presence of dyes does not change the overall picture of folding. At the same time, some deviations from folding of the original protein are observed, in particular, the FRET constructs fold considerably slower than the original protein because the protein collapse in the initial state of folding is slowed down due to the protein loading with relatively massive dyes.

1. Introduction

Protein folding is one of the fundamental challenges in molecular biology. The complexity of the problem is mostly due to the diversity of folding pathways, which are characterized by different sequences of protein states, different probabilities to occur and different folding times [1–9]. Particularly, experimental studies of folding dynamics and kinetics are difficult to perform, because they require close monitoring of individual protein molecules. One of the possible solutions to this problem is a single-molecule spectroscopy [10], in particular, the single-molecule Förster resonance energy transfer (smFRET) [11–13]. In this method, the efficiency of energy transfer between two dyes, donor and acceptor, depends on the inter-dye distance. By monitoring the energy transfer from donor to acceptor, one can determine how the distance between two loci of protein chain, to which the dyes are attached, varies in the course of folding. Currently, two dyes are typically

E-mail address: chekmarev@itp.nsc.ru.

https://doi.org/10.1016/j.bpc.2019.106243
Received 16 July 2019; Received in revised form 1 August 2019; Accepted 2 August 2019
Available online 09 August 2019

employed [14–18], although the smFRET experiments with three dyes have recently been performed, which gave a more informative picture of folding [19] (see also relevant multi-colour studies of conformational transitions in nucleic acids [20]).

A key question in the application of the smFRET technique to study protein folding is how the dyes affect the protein behavior. Understanding of these effects is particularly important for small proteins, for which the dyes, along with their linkers, can be comparable in size (mass) with the protein. Some aspects of this problem have been investigated using a coarse-grained model for a 86-residue four-helix bundle protein (Im7) [21]. The attention was mostly given to equilibrium properties, and it was found that, depending on the dye placement, the effect of the dyes may be significant, although the overall folding mechanism does not change. In the present paper, we also use a coarse-grained protein model to perform simulations. The model is less realistic than that in the above paper [21], but we study a wider spectrum of protein folding characteristics, i.e., not only the equilibrium properties, but also the folding kinetics and FRET histograms. As a characteristic, small protein, we consider BBL, which has been actively studied with the smFRET technique [14–17]. To represent the protein, a C_α-model with a Gō-like interaction potential was used, similar to that in the previous study of this protein [22]. In contrast to that study [22], the dyes and linkers were introduces explicitly, as the chains of beads of smaller (linkers) and larger (dyes) size. The process of protein folding was simulated with constant-temperature (Langevin's) molecular dynamics.

To determine the dye-protein interaction, we note that the attractive interaction, which accounts for possible dye sticking to the protein body, is residue specific [23–27] and requires an atomic-level consideration [23,27,28]. The repulsive interaction is not so specific and leads to the appearance of the excluded volume in the protein conformation space, which is roughly determined by the dye size and mobility, similar to the dye-accessible volume [29–31]. Therefore, due to their unspecific nature, the excluded volume effects are expected to be common for the FRET experiments. Motivated by this consideration, we assumed that the dyes and linkers interacted with each other and with the protein beads purely repulsively, similar to the previous coarse-grained modeling of smFRET experiments [21,32].

Three systems have been considered: the original protein, as a “baseline” no-dye model, and two FRET constructs. In the first construct, the dyes were attached to the protein termini, which is most common in the current smFRET experiments [14–17], and in the second FRET construct, in order to reveal a possible (“maximum”) effect of the dye placement on the process of folding, one of the dyes was attached to the residue that formed critical contacts in the transition state. The free energy surfaces, folding time distributions and FRET efficiency histograms were constructed based on the simulated folding trajectories. Overall, it has been found that despite the excluded-volume effect produced by the dyes, the attachment of the dyes do not change the overall picture of BBL folding, although some deviations from folding of BBL protein exist, e.g., the FRET constructs fold slower than the BBL protein.

The paper is organized as follows. Section 2 describes coarse-grained models of the systems and simulation method, Sect. 3 presents results and their discussion, and Sect. 4 summarizes the results and gives some concluding remarks.

2. System and simulation method

BBL is a 45-residue protein (QNNDALSPAIRRLLAEHNLDASAIKGTGVGGRLTREDVEKHLAKA, 1w4h.pdb) [33], which consists of two parallel α-helices and a short 3_{10} helix between them (Fig. 1**a**). To simulate FRET experiments, a coarse-grained model of the system was constructed, where the protein residues, linkers and dyes were represented by monomers (“beads”). The beads associated with the residues were centered at the C_α atoms, based on the NMR structure of the protein [33]. The linkers consisted of four beads of smaller size, and the dyes were represented by single beads of larger size [21]. For the protein, the interaction potential was chosen to be a Gō-like potential [34] in the form [35] that has been successfully used to simulate BBL folding [22].

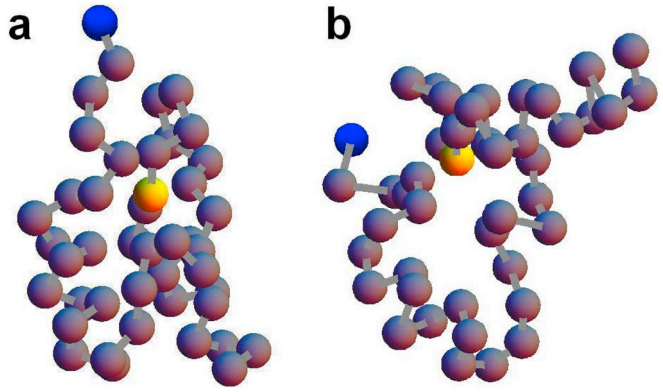

Fig. 1. Coarse-grained, C_α-structure of (**a**) the native structure of BBL (1w4h.pdb [33]), and (**b**) of a transition state of the protein. The blue colored bead is the N-terminal of the protein, and the yellow colored one represents the residue at which the number of contacts in the transition state differs most significantly from that in the native state (Fig. 3). (For interpretation of the references to colour in this figure legend, the reader is referred to the web version of this article.)

$$U = \sum_{i-1}^{N-1} [k_1(r_{i,i+1} - d_0^0)^2 + k_2(r_{i,i+1} - d_0^0)^4] + \sum_{i+1<j}^{\mathrm{NAT}} 4\varepsilon \left[\left(\frac{\sigma_{ij}^0}{r_{ij}} \right)^{12} - \left(\frac{\sigma_{ij}^0}{r_{ij}} \right)^6 \right] + \sum_{i+1<j}^{\mathrm{NON}} 4\varepsilon \left[\left(\frac{\sigma_0}{r_{ij}} \right)^{12} - \left(\frac{\sigma_0}{r_{ij}} \right)^6 + \frac{1}{4} \right] \Delta(r_{ij} - d_{\mathrm{nat}})$$

where N is the number of residues in the protein, r_{ij} is the current distance between monomers i and j, and ε is the attractive energy. The first term of the right-hand side of the equation accounts for the rigidity of protein backbone, with ${d_0}^0 = 3.8$Å, $k_1 = \varepsilon/$Å^2, and $k_2 = 100\varepsilon/$Å^4, and the second and third terms determine the contributions of native and non-native contacts, respectively. The monomers i and j were considered to be in native contact if $|j - i| > 1$ and the distance between them was less than r_{cut}, which was chosen to be large enough, $r_{\mathrm{cut}} = 9$Å, in order to take into account long-range native contacts that are essential for the formation of the native state [36]. The total number of native contacts in this case is equal to 193. In the second term ${\sigma_{ij}}^0 = 2^{-1/6} d_{ij}$, where d_{ij} is the distance between monomers i and j in the native state, and in the third term $d_{\mathrm{nat}} = \langle d_{ij} \rangle$, $\sigma_0 = 2^{-1/6} d_{\mathrm{nat}}$, and $\Delta(r_{ij} - d_{\mathrm{nat}})$ is the cutoff function which is equal to 1 for $r_{ij} < d_{\mathrm{nat}}$ and 0 otherwise. The linkers and dyes interacted with each other and with the protein beads purely repulsively [21,32], specifically as

$$U = \sum [k_1(r_{i,i+1} - d_0)^2 + k_2(r_{i,i+1} - d_0)^4] + \sum 4\varepsilon(\sigma_{ij}/r_{ij})^{12}$$

where in the first term of the right-hand side of the equation, the summation is taken over the bonds that connect the dye, linker and the protein residue to which the dye is attached, and in the second term, the summation covers all pairs of the contacts between the dye and linkers with the protein beads. To reproduce, by the order of magnitude, the size difference between the dyes and protein residues, the radii of the dyes were chosen to be $f_{\mathrm{dye}} = 1.7$ times larger that those of the residues, which corresponds to the difference in masses as 550 Da (dyes) to 110 Da (residues). The radii of the linkers were taken, rather arbitrarily, to be $f_{\mathrm{link}} = 0.8$ of the protein bead radii. Accordingly, in the above equation, when the linkers interacted with the protein beads, $d_0 = {d_0}^0(1 + f_{\mathrm{link}})/2$ and $\sigma_{ij} = {\sigma_{ij}}^0(1 + f_{\mathrm{link}})/2$, when with the dyes,

$d_0 = d_0^0(f_{dye} + f_{link})/2$ and $\sigma_{ij} = \sigma_{ij}^0(f_{dye} + f_{link})/2$, and when they interacted with each other, $d_0 = d_0^0 f_{link}$ and $\sigma_{ij} = \sigma_{ij}^0 f_{link}$. Correspondingly, for the interaction of the dyes with the protein beads, it was $d_0 = d_0^0(1 + f_{dye})/2$ and $\sigma_{ij} = \sigma_{ij}^0(1 + f_{dye})/2$, and for the interaction with each other $d_0 = d_0^0 f_{dye}$ and $\sigma_{ij} = \sigma_{ij}^0 f_{dye}$.

The simulations were performed using a constant-temperature MD based on the Langevin equation

$$m_i \frac{d^2\mathbf{r}_i}{dt^2} + \gamma \frac{d\mathbf{r}_i}{dt} = -\frac{\partial U}{\partial \mathbf{r}_i} + \Phi_i(t)$$

where m_i is the mass of i monomer, $\mathbf{r}_i$ is its radius-vector, U is the potential energy of the system, Φ_i are random forces from the surroundings, and γ is the coefficient of friction with the surroundings to balance random forces and dissipation. The dyes and linkers have, respectively, masses $f_{dye}^3 m_0$ and $f_{link}^3 m_0$, where $m_0 = 110$ Da is the characteristic residue mass. The random forces have the Gaussian distribution with zero mean and variance $\langle \Phi_i^j(t)\Phi_{i'}^{j'}(t+\tau)\rangle = 2\gamma T\delta_{ii'}\delta_{jj'}\delta(\tau)$, where T is the temperature, which is measured in the energy units ε (i.e., the Boltzmann constant is set to unity), the angular brackets denote an ensemble average, the upper index at Φ stands for the vector component, and $\delta_{kk'}$ and $\delta(\tau)$ are the Kronecker and Dirac delta functions, respectively. The equation was numerically integrated [37] with the time step $\Delta t = 0.0125\tau$ and $\gamma = 50m_0/\tau$ [38]. With the length scale $l = 9$Å and the characteristic attractive energy $\varepsilon \approx 2.2$kcal/mol [39], the characteristic time scale $\tau = (m_0 l^2/\varepsilon)^{1/2}$ is ≈3ps.

3. Results and discussion

3.1. The FRET constructs

Two different FRET constructs were considered. In one, the dyes were attached to the beads corresponding to protein termini, as in Fig. 2a, which is typical of the FRET experiments on protein folding [14–18]. The other FRET construct was intended to reveal a possible ("maximum") effect of the dye placement on the process of protein folding. To create it, the transition state conformations of BBL were analyzed, and the key residue that formed critical contacts was determined [40,41]. To find the transition state conformations, various protein states were taken from the transition state region [42], which served as the starting points to perform the pfold analysis [43]. Specifically, 20 MD trajectories, with slightly different bead velocity distributions, were started in each state and run until a native-like state ($\sigma_{nat} < 2.5$Å) or an unfolded state ($\sigma_{nat} > 8$Å) was achieved, where σ_{nat} is the root-mean-square-deviation (RMSD) from the native state. The current state was considered to be a transition state if the number of trajectories reaching the native-like state varied from 9 to 11. In this way, 50 transition states, very close to each other, were found (Fig. 1b).

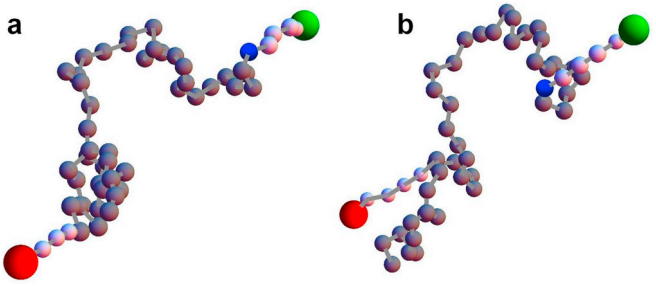

Fig. 2. The extended conformations of the FRET constructs at which the simulations were started: with the dyes attached (**a**) to the protein termini, and (**b**) to the N-terminus and residue No. 33. The dark-gray beads represent the protein residues (with the N-terminal residue shown in blue), the light-gray beads are for the linkers, and the green and red beads represent the dyes. (For interpretation of the references to colour in this figure legend, the reader is referred to the web version of this article.)

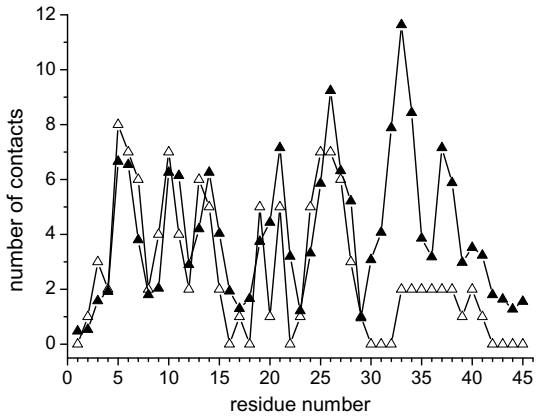

Fig. 3. The numbers of contacts that the residues have in the native state (empty triangles) and in the transition state (solid triangles).

They were used to calculate the average number of contacts $\langle N_i\rangle^{TSE}$ that i residue has in the transition state (Fig. 3). The comparison of $\langle N_i\rangle^{TSE}$ with the corresponding numbers of contacts for the native state N_i^{nat} (Fig. 3) reveals that the key residue is the one of number 33, for which $\phi_i = \langle N_i\rangle^{TSE}/N_i^{nat}$ is maximal (for the existing native contacts). Accordingly, in the second FRET construct, one dye was attached to the bead for the N-terminus of the protein, and other to the bead representing the residue number 33, as in Fig. 2**b**.

3.2. Folding kinetics

The MD trajectories were started in unfolded states of the protein and terminated upon reaching the natives state. The unfolded states for the FRET constructs are shown in Fig. 2; the unfolded state for the original protein (not shown) was the same, except that no dyes were attached. The native state of the protein was considered to be reached when the RMSD from the native state $\sigma_{nat} < 1$Å. Folded structures of the FRET constructs are depicted in Fig. 4. In each case, 10^3 trajectories were run at a temperature $T = 0.275$ measured in the energy units ε; with $\varepsilon \approx 2.2$kcal/mol [39], it is equal to approximately 300 K. Fig. 5 shows the protein state probability surfaces depending on the fraction of native contacts (f_{nat}) and the radius of gyration (R_g), with the latter calculated over the beads representing the protein. The surfaces are presented in the form of free energy surfaces (FESs), which is a common representation for protein folding studies. The free energy was calculated as.

$$F(f_{nat}, R_g) = -T \ln P(f_{nat}, R_g)$$

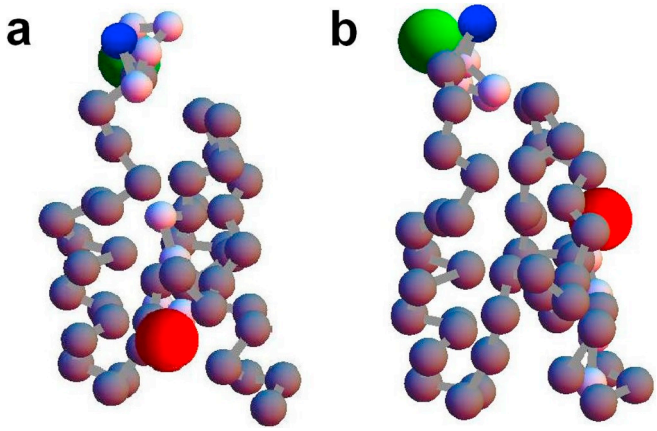

Fig. 4. Folded structures of the FRET constructs (**a**) with the dyes at the protein termini, and (**b**) with the dyes at the protein N-terminus and residue No. 33.

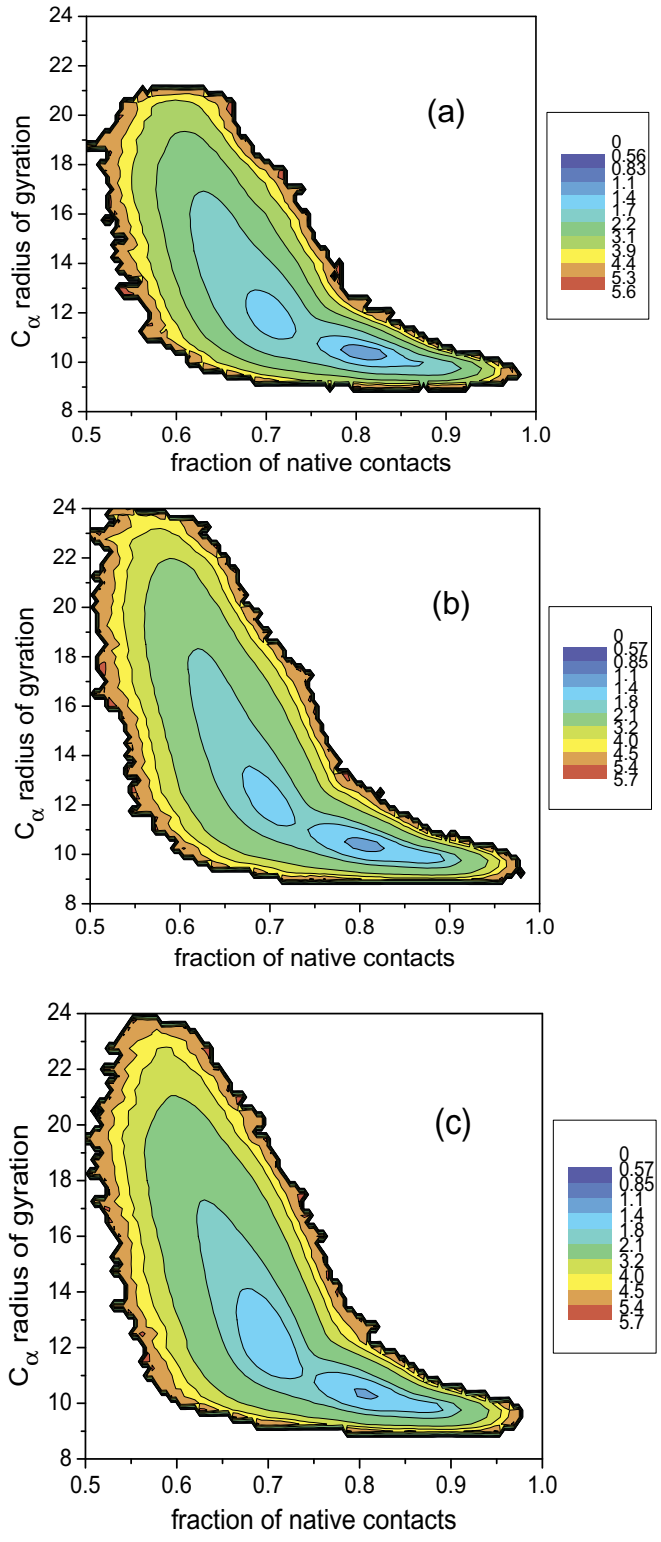

Fig. 5. Free energy surfaces for the first-passage folding trajectories: (**a**) no dyes, (**b**) dyes at the protein termini, and (**c**) dyes at the protein N-terminus and residue No. 33. The radius of gyration is measured in angstroms.

where $P(f_{nat},R_g)$ is the probability for the system to be found at the point (f_{nat},R_g). All FESs are very similar except that the radius of gyration in the initial stage folding in the surfaces for the FRET constructs is larger than that in the surface for the original protein. This suggests that the protein collapse is slowed down due to the dye loading. All surfaces reveal two basins of attraction, one for semi-compact states (at $f_{nat} \approx 0.7$), and the other for native-like states (larger values of f_{nat}), which suggests two-state folding kinetics. The basins are separated by relatively low barriers, i.e., the BBL folding in our simulations is marginally barrier-limited [15] rather than downhill [16,17]. This is confirmed by the first-passage time distributions, which are single-exponential; they are shown in Fig. 6 in the form of survival probabilities. The mean first-passage times (MFPTs) for the FRET constructs are very close to each other (equal to $\approx 1.1 \times 10^4$) and larger than the MPFT for the original protein ($\approx 0.7 \times 10^4$). This is in agreement with the above mentioned difference in the FESs for these systems, i.e., that the larger values of radius of gyration for the FRET constructs in the initial stage of protein folding indicate that the attachment of the dyes slows the folding process.

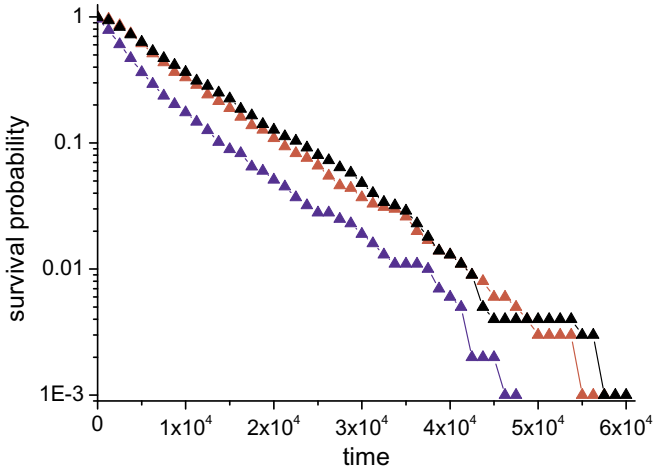

Fig. 6. First-passage time distributions in the form of survival probabilities: no dyes (blue), the dyes at the protein termini (black), and the dyes at the protein N-terminus and residue No. 33 (red). Time is measured in units of the characteristic time τ (Sect. 2). (For interpretation of the references to colour in this figure legend, the reader is referred to the web version of this article.)

3.3. Equilibrium folding and FRET histograms

To mimic equilibrium folding, one hundred MD trajectories were run starting at the unfolded states of the system depicted in Fig. 2. The trajectories were continued for 10^6 time steps, which was sufficient [22] to reproduce the FESs obtained with all-atom simulations in explicit solvent [44,45]. At this lengths of the trajectories, approximately 75% (the FRET constructs) to 90% (the original protein) of folding events were covered (Fig. 6). The ensemble of the trajectories was used instead of one long trajectory in order to avoid a possible dependence of the results on the initial (seed) random number when different systems are compared. Fig. 7 shows FESs for the original protein (panel **a**) and FRET constructs (panels **b-c**). The surfaces are similar to those for the "first-passage folding" (Fig. 5). In particular, in that in the initial stage of folding, the FRET constructs are less compact than the original protein. The primary difference between Figs. 5 and 7 is that the basin for native-like states that was situated at $f_{nat} \approx 0.8$ in the former case shifts to larger values of f_{nat} (≈ 0.87), in good agreement with the FES for all-atom simulations in explicit solvent [45]. This is because in the latter case the trajectories were not terminated upon reaching the native state, allowing the protein to explore native-like states further.

Fig. 8 presents FRET efficiency histograms for the FRET construct with the dyes attached to the protein termini, which is typical of the FRET experiments on protein folding [14–18] and has been found most informative in comparison with the other dye placements [22]. The efficiency of energy transfer is determined as

$$E(r) = 1/[1 + (r/R_0)^6] \quad (1)$$

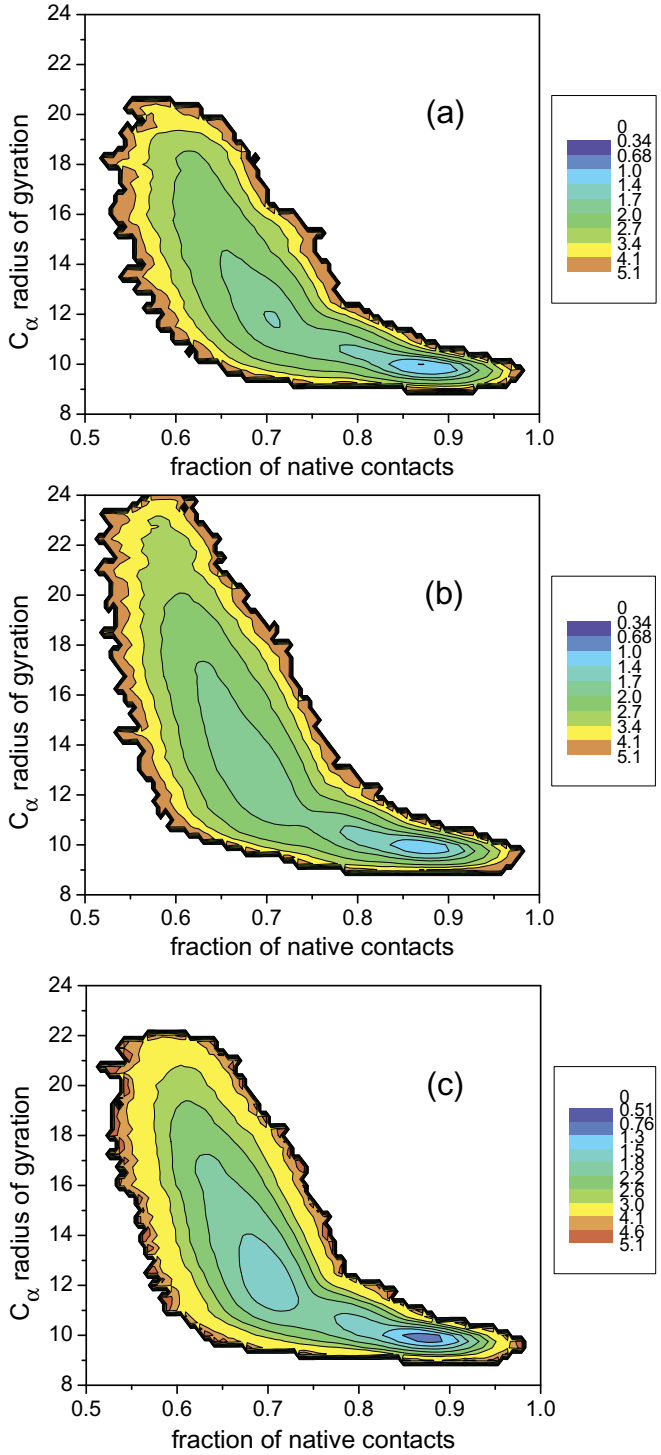

Fig. 7. Free energy surfaces for the equilibrium folding conditions: (**a**) no dyes, (**b**) dyes at the protein termini, and (**c**) dyes at the protein N-terminus and residue No. 33. The radius of gyration is measured in angstroms.

where r is the distance between the dyes, and R_0 is the Förster radius, at which the efficiency is 50%. Small values of the efficiency are associated with unfolded states of the protein, because the inter-dye distances in such states are expected to be large, and large values of the efficiency are associated with folded states, in which the inter-dye distances are expected to be small. Since the FRET efficiency depends on the ratio between the inter-dye distance and the Förster radius [Eq. (1)], the change of the range of the inter-dye distances is equivalent to the change of the Förster radius. Then, taking into account that the

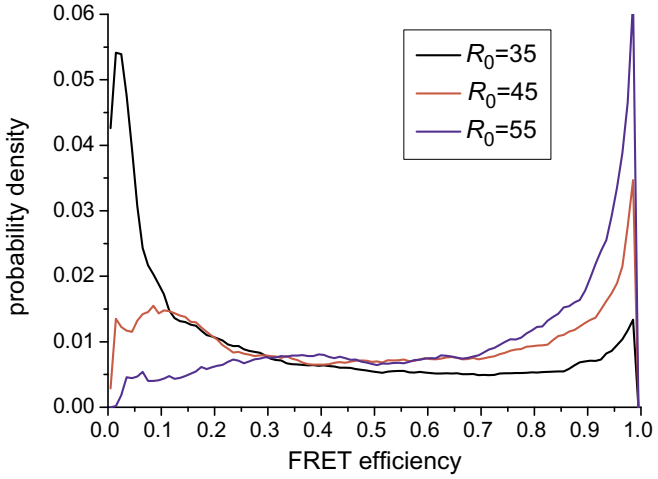

Fig. 8. FRET-efficiency histograms for different values of the Förster radius R_0.

folding kinetics are two-state (Fig. 6), i.e., only two characteristic states were observed - unfolded and folded (Fig. 7), the variation of the Förster radius can be used to mimic how the population of these states changes with the denaturant concentration [22]. Fig. 8 shows the histograms for three values of the Förster radius. $R_0 = 45$ represents an "optimal" value of the Förster radius (R_0^{opt}); it is equal to one-half of the maximum inter-dye distance, which is ≈90Å in the present simulations. At this value of R_0, both unfolded and folded states are present in the histogram, which are represented by peaks at low and large values of E, respectively. If R_0 is taken to be smaller than R_0^{opt}, the existing inter-dye distances are effectively enlarged in Eq. (1), as if the protein would be mostly in unfolded state. Accordingly, the peak at low value of E increases, and that at large value of E decreases. On the contrary, if R_0 is taken to be larger than R_0^{opt}, the inter-dye distances are effectively shortened, as if the protein would be mostly in folded state. This changes the histogram in the opposite way, i.e., the peak at low value of E decreases, and that at large value of E increases. Based on this reasoning, the pattern of the FRET histogram will change with denaturant concentration as follows (Fig. 8). At high denaturant concentrations, the protein is mostly unfolded, so that the histogram will be similar to that at $R_0 = 35$, where the peak at E close to zero dominates. At moderate denaturant concentrations, both unfolded and folded states are expected to be present. Then, the histogram at $R_0 = 45$ will be more representative, where the peaks at small and large values of E are comparable in value. Finally, when the denaturant concentration becomes low, the protein will be found mostly in the folded state. In this case, the histogram at $R_0 = 55$, in which one peak is observed at $E = 1$, will be characteristic. The present picture of evolution of the FRET histograms with denaturant concentration is in good agreement with the smFRET experiments on BBL folding [15,17] in that the increase of the denaturant concentration (0 to 6 M GdmCl [15], and 0.2 M to 8 M urea [17]) lowers the peak corresponding to the native conformations and raises the peak for the denatured states [15,17].

4. Conclusions

The goal of the present work was to examine how the dyes that are attached to the proteins in the smFRET experiments influence protein behavior during folding. This question is of particular importance for small proteins, for which the dyes, along with their linkers, can be comparable in size (mass) with the protein. In comparison to the previous studies, we have considered a wider spectrum of protein folding characteristics, i.e., not only the equilibrium properties [21], but also the folding kinetics and FRET histograms. As a characteristic system, we employed BBL protein, which has been actively studied with the smFRET measurements [14–17]. To be able to consider all properties of

interest, a coarse-grained description of the original protein and two FRET constructs were employed. Specifically, for the protein, a C_α-model with a Gō-like interaction potential was used. The dyes and linkers in the FRET constructs were introduced explicitly, i.e., the dyes were represented by single beads of larger size (in comparison with the beads representing the protein residues), and the linkers were modeled by the chains of four beads of smaller size. The dyes and linkers interacted with each other and with the protein beads purely repulsively. The process of protein folding was simulated with constant-temperature (Langevin's) molecular dynamics.

Three systems have been considered: the original protein, as a "baseline" no-dye model, and two FRET constructs. In one construct, the dyes were attached to the protein termini, as is usually done in the FRET experiments [14–17]. The second construct was created in order to reveal a possible ("maximum") effect of the dye placement on the process of protein folding. For this purpose, using a pfold analysis, the key residue that formed critical contacts in the transition state was determined (residue number 33), and one dye was attached to the N-terminus of the protein, and the other to that residue. To study folding kinetics, the MD trajectories were started at an unfolded state of the protein and terminated upon reaching the native state. It was found, a bit surprisingly, that the residence probability surfaces for the original protein and FRET constructs are very similar. Not only each of the surfaces, presented in the form of a free energy surface, has two characteristic basins - one for semi-compact states, and the other for native-like states - but also these basins are positioned very similarly on the surfaces. It was also observed that the FRET constructs remain less compact than the original protein in the initial (collapse) stage of folding, which indicates that the dyes slow down folding. The three systems produced similar, exponential distributions of the first-passage times, which is in agreement with the observed structure of the FESs. This suggests that the addition of the dyes does not change the folding kinetics in general, i.e., the kinetics remain two-state, as for the original protein. The MFPTs for the FRET constructs are very close to each other and larger than that for the original protein (by approximately 1.6 times), which is in the line with the above mentioned dye mediated collapse of the FRET constructs. The true FESs, obtained with quasi-equilibrium simulations, have been found similar to the above "non-equilibrium" ones, except that the basins for native-like states shifted toward the native state. This is because the MD trajectories were not terminated upon reaching the native state, which allowed the system to explore the native-like states further. To mimic evolution of the FRET efficiency histograms with denaturant concentration, the histograms for different values of the Förster radius have been calculated and found in agreement with experimental results in that the increase of the denaturant concentration lowers the peak corresponding to the native conformations and raises the peak for the denatured states [15,17].

In general, the obtained results suggest that even for small proteins, such as 45-residue BBL, the appearance of the excluded volume in the protein conformation space due to the presence of dyes does not change the overall picture of folding, which is in agreement with the previous study of the 86-residue protein Im7 [21]. At the same time, some deviations from folding of the original BBL protein are observed. In particular, the FRET constructs fold considerably slower than the original protein because the protein collapse in the initial state of folding is slowed down due to the protein loading with massive dyes.

Acknowledgement

This work was supported by a grant from the Russian Foundation for Basic Research (18-04-00013).

References

[1] A.R. Dinner, A. Šali, L.J. Smith, C.M. Dobson, M. Karplus, Understanding protein folding via free-energy surfaces from theory and experiment, Trends Biochem. Sci. 25 (2000) 331–339.
[2] J.N. Onuchic, Z. Luthey-Schulten, P.G. Wolynes, Theory of protein folding: the energy landscape perspective, Annu. Rev. Phys. Chem. 48 (1997) 545–600.
[3] W.A. Eaton, V. Muñoz, S.J. Hagen, G.S. Jas, L.J. Lapidus, E.R. Henry, J. Hofrichter, Fast kinetics and mechanisms in protein folding, Annu. Rev. Biophys. Biomol. Struct. 29 (2000) 327–359.
[4] J.-E. Shea, C.L. Brooks III, From folding theories to folding proteins: a review and assessment of simulation studies of protein folding and unfolding, Annu. Rev. Phys. Chem. 52 (2001) 499–535.
[5] K.A. Dill, S.B. Ozkan, M.S. Shell, T.R. Weikl, The protein folding problem, Annu. Rev. Biophys. 37 (2008) 289–316.
[6] K. Lindorff-Larsen, S. Piana, R.O. Dror, D.E. Shaw, How fast-folding proteins fold, Science 334 (2011) 517–520.
[7] H. Gelman, M. Gruebele, Fast protein folding kinetics, Q. Rev. Biophys. 47 (2014) 95–142.
[8] S. Gianni, P. Jemth, Protein folding: vexing debates on a fundamental problem, Biophys. Chem. 212 (2016) 17–21.
[9] V. Muñoz, M. Cerminara, When fast is better: protein folding fundamentals and mechanisms from ultrafast approaches, Biochem. J. 473 (2016) 2545–2559.
[10] S. Weiss, Fluorescence spectroscopy of single biomolecules, Science 283 (1999) 1676–1683.
[11] B. Schuler, H. Hofmann, Single-molecule spectroscopy of protein folding dynamics-expanding scope and timescales, Curr. Opin. Struct. Biol. 23 (2013) 36–47.
[12] H.S. Chunga, I.V. Gopich, Fast single-molecule FRET spectroscopy: theory and experiment, Phys. Chem. Chem. Phys. 16 (2014) 18644–18657.
[13] E. Lerner, T. Cordes, A. Ingargiola, Y. Alhadid, S.-Y. Chung, X. Michalet, S. Weiss, Toward dynamic structural biology: two decades of single-molecule Förster resonance energy transfer, Science 359 (2018) eaan1133.
[14] M. Sadqi, L.J. Lapidus, V. Muñoz, How fast is protein hydrophobic collapse? Proc. Natl. Acad. Sci. U. S. A. 100 (2003) 12117–12122.
[15] F. Huang, L. Ying, A.R. Fersht, Direct observation of barrier-limited folding of BBL by single-molecule fluorescence resonance energy transfer, Proc. Natl. Acad. Sci. U. S. A. 106 (2009) 16239–16244.
[16] L.A. Campos, J. Liu, X. Wang, R. Ramanathan, D.S. English, V. Muñoz, A photoprotection strategy for microsecond-resolution single-molecule fluorescence spectroscopy, Nat. Methods 8 (2011) 143–146.
[17] J. Liu, L.A. Campos, M. Cerminara, X. Wang, R. Ramanathan, D.S. English, V. Muñoz, Exploring one-state downhill protein folding in single molecules, Proc. Natl. Acad. Sci. U. S. A. 109 (2012) 179–184.
[18] H.S. Chung, W.A. Eaton, Protein folding transition path times from single molecule FRET, Curr. Opin. Struct. Biol. 48 (2018) 30–39.
[19] J. Yoo, J.M. Louis, I.V. Gopich, H.S. Chung, Three-color single-molecule FRET and fluorescence lifetime analysis of fast protein folding, J. Phys. Chem. B 122 (2018) 11702–11720.
[20] R.A. Riskowski, R.E. Armstrong, N.L. Greenbaum, G.F. Strouse, Triangulating nucleic acid conformations using multicolor surface energy transfer, ACS Nano 10 (2016) 1926–1938.
[21] L.R. Allen, E. Paci, Simulation of fluorescence resonance energy transfer experiments: effect of the dyes on protein folding, J. Phys. Condens. Matter 22 (2010) 235103.
[22] V.A. Andryushchenko, S.F. Chekmarev, Modeling of multicolor single-molecule Förster resonance energy transfer experiments on protein folding, J. Phys. Chem. B 122 (2018) 10678–10685.
[23] A.C. Vaiana, H. Neuweiler, A. Schulz, J. Wolfrum, M. Sauer, J.C. Smith, Fluorescence quenching of dyes by tryptophan: interactions at atomic detail from combination of experiment and computer simulation, J. Am. Chem. Soc. 125 (2003) 14564–14572.
[24] S. Doose, H. Neuweiler, M. Sauer, A close look at fluorescence quenching of organic dyes by tryptophan, ChemPhysChem 6 (2005) 2277–2285.
[25] M. Hoefling, N. Lima, D. Haenni, C.A.M. Seidel, B. Schuler, H. Grubmüller, Structural heterogeneity and quantitative FRET efficiency distributions of Polyprolines through a hybrid atomistic simulation and Monte Carlo approach, PLoS One 6 (2011) e19791.
[26] D. Haenni, F. Zosel, L. Reymond, D. Nettels, B. Schuler, Intramolecular distances and dynamics from the combined photon statistics of single-molecule FRET and photoinduced electron transfer, J. Phys. Chem. B 117 (2013) 13015–13028.
[27] R.B. Best, H. Hofmann, D. Nettels, B. Schuler, Quantitative interpretation of FRET experiments via molecular simulation: force field and validation, Biophys. J. 108 (2015) 2721–2731.
[28] K. Claridge, A. Troisi, Developing consistent molecular dynamics force fields for biological chromophores via force matching, J. Phys. Chem. B 123 (2019) 428–438.
[29] A. Muschielok, J. Andrecka, A. Jawhari, F. Brückner, P. Cramer, J. Michaelis, A nano-positioning system for macromolecular structural analysis, Nat. Methods 5 (2008) 965–971.
[30] S. Sindbert, S. Kalinin, H. Nguyen, A. Kienzler, L. Clima, W. Bannwarth, B. Appel, S. Müuller, C.A.M. Seidel, Accurate distance determination of nucleic acids via Föorster resonance energy transfer: implications of dye linker length and rigidity, J. Am. Chem. Soc. 133 (2011) 2463–2480.
[31] K. Walczewska-Szewc, B. Corry, Accounting for dye diffusion and orientation when relating FRET measurements to distances: three simple computational methods, Phys. Chem. Chem. Phys. 16 (2014) 12317–12326.
[32] K.A. Merchant, R.B. Best, J.M. Louis, I.V. Gopich, W.A. Eaton, Characterizing the unfolded states of proteins using single-molecule FRET spectroscopy and molecular simulations, Proc. Natl. Acad. Sci. U. S. A. 104 (2007) 1528–1533.
[33] N. Ferguson, T.D. Sharpe, P,.J. Schartau, S. Sato, M.D. Allen, C.M. Johnson, T.J. Rutherford, A.R. Fersht, Ultra-fast barrier-limited folding in the peripheral

subunit-binding domain family, J. Mol. Biol. 353 (2005) 427–446.
[34] N. Gō, Theoretical studies of protein folding, Annu. Rev. Biophys. Bioeng. 12 (1983) 183–210.
[35] T.X. Hoang, M. Cieplak, Molecular dynamics of folding of secondary structures in go-type models of proteins, J. Chem. Phys. 112 (2000) 6851–6862.
[36] S.S. Cho, P. Weinkam, P.G. Wolynes, Origins of barriers and barrierless folding in BBL, Proc. Natl. Acad. Sci. U. S. A. 105 (2008) 118–123.
[37] R. Biswas, D.R. Hamann, Simulated annealing of silicon atom clusters in Langevin molecular dynamics, Phys. Rev. B 34 (1986) 895–901.
[38] D.K. Klimov, D. Thirumalai, Viscosity dependence of the folding rates of proteins, Phys. Rev. Lett. 79 (1997) 317–320.
[39] S. Miyazawa, R.L. Jernigan, Residue-residue potentials with a favorable contact pair term and an unfavorable high packing density term, for simulation and threading, J. Mol. Biol. 256 (1996) 623–644.
[40] A. Li, V. Daggett, Characterization of the transition state of protein unfolding by use of molecular dynamics: chymotrypsin inhibitor 2, Proc. Natl. Acad. Sci. U. S. A. 91 (1994) 10430–10434.
[41] M. Vendruscolo, E. Paci, C.M. Dobson, M. Karplus, Three key residues form a critical contact network in a protein folding transition state, Nature 409 (2001) 641–645.
[42] N.V. Dokholyan, S.V. Buldyrev, H.E. Stanley, E.I. Shakhnovich, Identifying the protein folding nucleus using molecular dynamics, J. Mol. Biol. 296 (2000) 1183–1188.
[43] R. Du, V.S. Pande, A.Yu. Grosberg, T. Tanaka, E.I. Shakhnovich, On the transition coordinate for protein folding, J. Chem. Phys. 108 (1998) 334–350.
[44] J. Zhang, W. Li, J. Wang, M. Qin, W. Wang, All-atom replica exchange molecular simulation of protein BBL, Proteins Struct. Funct. Bioinform. 72 (2008) 1038–1047.
[45] Z. Yue, J. Shen, pH-dependent cooperativity and existence of a dry molten globule in the folding of a miniprotein BBL, Phys. Chem. Chem. Phys. 20 (2018) 3523–3530.